Urban $PM_{2.5}$ at Realistic Environmental Concentrations Impairs Blood–Brain Barrier Integrity and Enhances LOX-1 Expression in Human Brain Endothelial Cells

Elisabet Andersson[1], Trevor Wendt[1], Fanny Bergman[2], Christina Isaxon[2,3], Saema Ansar[1,*]

[1] Applied Neurovascular Research, Neurosurgery, Department of Clinical Sciences, Faculty of Medicine, Lund University, Lund, Sweden

[2] Ergonomics and Aerosol Technology, Department of Design Sciences, Faculty of Engineering, Lund University, Lund, Sweden

[3] NanoLund, Lund University, Lund, Sweden

*Corresponding author is Saema Ansar (Saema.Ansar@med.lu.se)

Keywords: Air pollution; $PM_{2.5}$; Blood-Brain Barrier; LOX-1; Human Brain Endothelial Cells, Ischemia

Highlights

- Urban $PM_{2.5}$ (15 μg/m^3) disrupts BBB integrity in human brain endothelial cells
- $PM_{2.5}$ induces endothelial dysfunction resembling ischemic-like injury
- Urban $PM_{2.5}$ (15 μg/m^3) exposure upregulates cardiovascular disease biomarker LOX-1
- A majority of the global population are exposed to BBB-disrupting $PM_{2.5}$ levels
- Vascular endothelial- and BBB dysfunction enhances risk for cerebrovascular disease

Graphical abstract

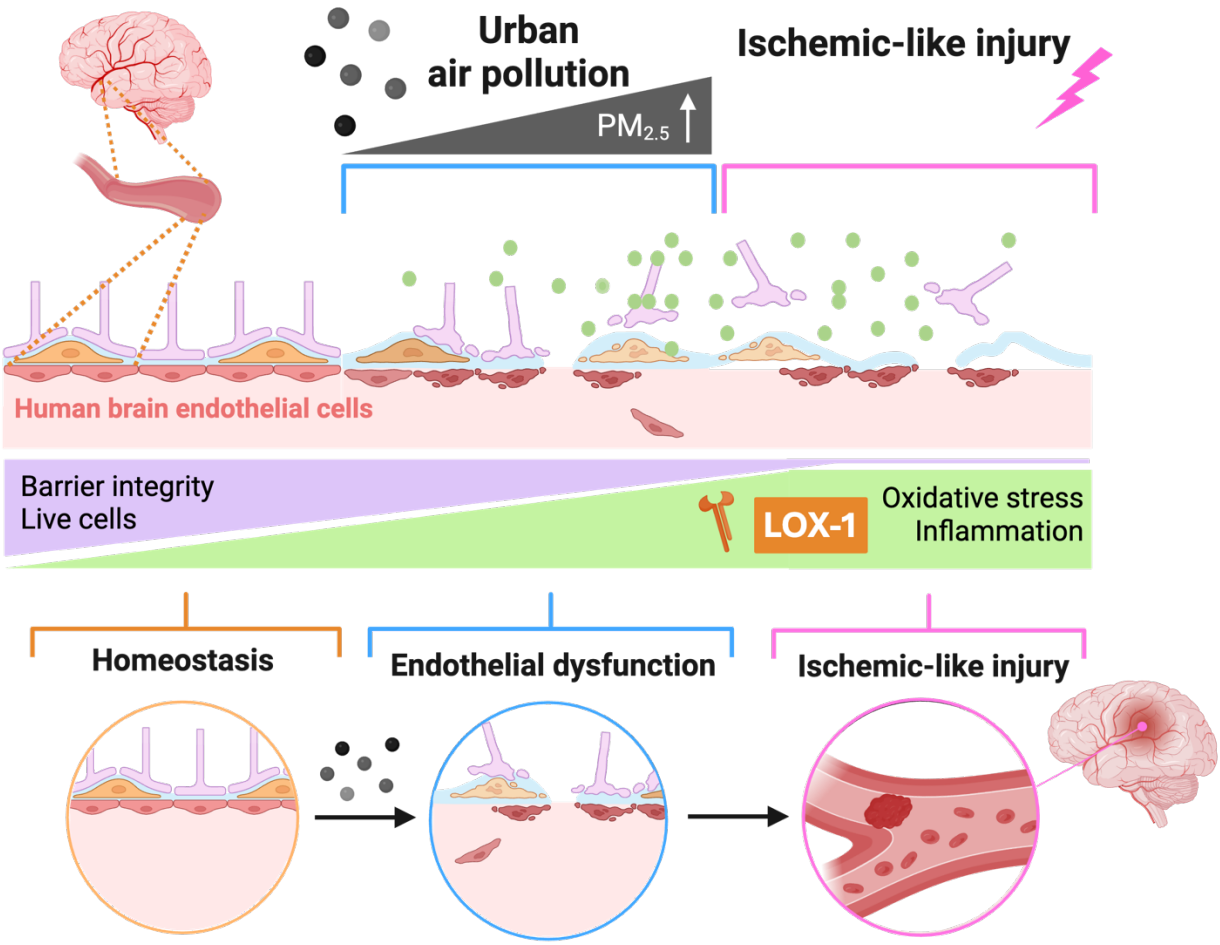

Abstract

Introduction

Ambient air pollution, especially fine particulate matter 2.5 ($PM_{2.5}$) has emerged as a critical environmental risk factor for cerebrovascular diseases, contributing to an estimated 7.9 million premature deaths annually. $PM_{2.5}$ induces cellular toxicity and is hypothesized to disrupt the blood-brain barrier (BBB), a pathological hallmark in cerebrovascular diseases such as ischemic stroke. Despite epidemiological evidence linking $PM_{2.5}$ to increased stroke incidence, its underlying cellular mechanism driving this association is poorly understood. It remains unclear how environmentally relevant pollution concentrations affects brain endothelial function or influence stroke-related biomarkers such as the lectin-like oxLDL receptor 1 (LOX-1).

Method

Primary adult male human brain microvascular endothelial cells (HBMEC) were exposed to $PM_{2.5}$ (5, 15, 75, or 300 μg/m^3) collected from an urban environment in southern Sweden, or control. Thereafter, exposed to normoxia (21% O_2) or hypoxia (1% O_2) and glucose deprivation, followed by reperfusion as a model for ischemic stroke. Cell viability, oxidative stress, inflammation, BBB integrity (claudin-5, ZO-1) and LOX-1 protein expression were assessed.

Results

$PM_{2.5}$ exposure induced cellular dysfunction, oxidative stress and inflammation starting at 75 μg/m^3 $PM_{2.5}$. Notably, decreased claudin-5 and ZO-1 protein levels and increased LOX-1 expression at concentrations as low as 15 μg/m^3 $PM_{2.5}$, levels commonly encountered in urban environments globally. The cellular effects of $PM_{2.5}$ closely resembled those induced by ischemic-like injury.

Conclusion

These findings demonstrate dose-dependent detrimental effects of $PM_{2.5}$ on HBMEC. The results suggest that ambient urban $PM_{2.5}$ may act as a predisposing factor for cerebrovascular disease onset, by causing endothelial and barrier dysregulation.

1. Introduction

Air pollution is widely recognized as the most significant environmental health risk globally, contributing to more than 7.9 million premature deaths annually (WHO, 2024, HEI, 2025). New safety guidelines for airborne particles with an aerodynamic diameter < 2.5 µm ($PM_{2.5}$) were established by the World Health Organisation (WHO) in 2021 to mitigate their adverse health impacts (WHO, 2021). However, despite these updated recommendations the WHO annual maximum limit of 5 µg/m^3 for ambient $PM_{2.5}$ is exceeded for more than 99% of the global population (WHO, 2021, WHO, 2022). $PM_{2.5}$ has emerged as a major risk factor for adverse health outcomes and is linked to development of respiratory, cardiovascular, cancer and neurodegenerative diseases. Strong epidemiological evidence demonstrates that elevated $PM_{2.5}$ exposure contributes to cardiovascular diseases with high mortality and societal burden including stroke, myocardial infarction and atherosclerosis (Krittanawong et al., 2023). In addition, $PM_{2.5}$ exposure is associated with both the onset and progression of neurodegenerative diseases such as Alzheimer's disease that has a substantial impact on quality of life (Lee et al., 2023, Best Rogowski et al., 2025, Huang et al., 2025). Despite the widespread exposure and strong epidemiological associations with health effects relating to the brain, significant gaps remain in understanding the underlying cellular mechanisms through which $PM_{2.5}$ contribute to disease. A major limitation in current toxicological research is the frequent use of $PM_{2.5}$ concentrations starting around 100 µg/m^3 (Kang et al., 2025, Chen et al., 2017, Zhu et al., 2018, Qin et al., 2023), which is far above the ambient concentrations encountered by majority of the global population. Consequently, little is known about effects of the lower, yet relevant, doses at which $PM_{2.5}$ begins to exert harmful effects. Furthermore, it is rarely addressed how much $PM_{2.5}$ reaches the brain upon inhalation exposure or how these particles affect brain vasculature as a large portion of pollution research focuses predominantly on the respiratory system. An additional methodological concern is that particles used in experimental studies are seldom collected from real urban environments and thereby do not accurately reflect the complex composition of air pollution particles which one is exposed to in daily life. These limitations create a substantial gap in generalizability and translational relevance of $PM_{2.5}$ toxicity research.

Given their small aerodynamic diameter, $PM_{2.5}$ particles can penetrate the lung epithelial barrier upon inhalation, enter the systemic bloodstream circulation and cross the blood-brain barrier (BBB) (Kang et al., 2021, Li et al., 2022). They may also reach the cerebral vasculature directly via the nasal cavity, reaching the olfactory bulb (Oberdorster et al., 2004). The BBB is a highly selective barrier which lines the cerebral vasculature and consists of endothelial cells preserved by tight junction proteins, such as claudin-5 and zonula occludens-1 (ZO-1) (Kadry et al., 2020). The barrier regulates the exchange of molecules between the blood and the brain which is crucial to maintain neural function and to protect the brain from toxins. The endothelial cells line the inner surface of blood vessels and are thereby the first point of contact between substances in the blood circulation and the BBB. Air pollution is therefore hypothesized to directly affect BBB function, and studies indicate that particle exposure can degrade tight-junction proteins and compromise barrier integrity (Oppenheim et al., 2013). $PM_{2.5}$ also induce oxidative stress by generating reactive oxygen species (ROS) in the respiratory and vascular

system, specifically in endothelial cells (Cui et al., 2015, Chen et al., 2017). Additionally, $PM_{2.5}$ activates the immune system by promoting the release of pro-inflammatory cytokines, ultimately contributing to neuroinflammation and neurodegeneration (Gu et al., 2022, Kang et al., 2021). Endothelial dyshomeostasis and loss of barrier integrity increases barrier permeability which allows for infiltration of inflammatory cells and toxins from the blood to the brain (Takata et al., 2021). This mechanism may then augment the $PM_{2.5}$-induced pathology through further inflammatory responses. As vascular endothelial cells represent the initial point of contact for circulating $PM_{2.5}$, their responses to particle exposure are highly relevant for cerebrovascular diseases.

The pathological features of air pollution on the vasculature closely resemble those observed in ischemic stroke, and accordingly, air pollution is estimated to be the second most prominent risk factor for stroke development (Collaborators, 2024). Ischemic stroke, caused by cerebral blood vessel occlusion which deprives neurons of oxygen and nutrients, leads to ROS and pro-inflammatory activation (Campbell et al., 2019, Gulke et al., 2018), causing endothelial damage and BBB degradation (Campbell et al., 2019). The lectin-like oxLDL receptor 1 (LOX-1) is upregulated in the acute phase of ischemic stroke and other cardiovascular pathologies, promoting downstream pro-inflammatory effects (Crucet et al., 2013, Arkelius et al., 2024). LOX-1 is linked to cerebrovascular endothelial dyshomeostasis and increased BBB permeability (Sawamura et al., 1997, Liang et al., 2020). Despite similarities in pathophysiology, the effects of $PM_{2.5}$ on stroke-linked pathogenic hallmarks are yet to be studied in the brain vasculature.

Given that $PM_{2.5}$ contributes to millions of premature deaths annually, elucidating the underlying pathological mechanism by which physiologically relevant concentrations of $PM_{2.5}$ causes damage to the brain endothelium is crucial for disease prevention and mortality reduction. The aim of this study was to investigate the effects of urban $PM_{2.5}$ on human brain microvascular endothelial cells (HBMEC) at concentrations reflecting WHO guidelines and real-world atmospheric exposure levels. The study examined cell viability, oxidative stress, inflammation, BBB integrity and LOX-1 expression as a stroke-linked pathogenic marker. To contextualize $PM_{2.5}$-induced effects, the outcomes were compared to an established *in vitro* model of ischemic stroke. The effects of prior $PM_{2.5}$ exposure on ischemic like injury outcome was also evaluated. This research addresses a critical gap in understanding how physiologically relevant concentrations of $PM_{2.5}$ induce cerebrovascular damage at the molecular and cellular level.

2. Materials and methods

2.1 Global urban $PM_{2.5}$ concentrations across cities as reference data for experimental concentration selection

To set environmentally realistic doses for *in vitro* exposure, data of hourly levels- and annual average $PM_{2.5}$ concentrations, was extracted from IQAir 2024 world air quality report and IQAir live hourly $PM_{2.5}$ measurement on website iqair.com. Annual averages were collected for Los Angeles (USA), São Paulo (Brazil), London (UK), Malmö (Sweden), Kinshasa (Democratic Republic of the Congo), Delhi (India), Beijing (China) and Sydney (Australia). Hourly fluctuation data was collected for Los Angeles, London, Malmö and Delhi at 09:00, 12:00, 17:00 and 00:00 on November 9th and November 10th of 2025. Different cities were selected to represent the biggest continents of the world, and to include Malmö where the studied particles were collected.

2.2 $PM_{2.5}$ collection and characterisation

Urban air pollution particles were collected near a street crossing in central Malmö according to previous study protocols (Bergman et al., 2024). Briefly, $PM_{2.5}$ was obtained using a high-volume impactor (900 l/min) (BGI900) which collected all particles < 2.5 µm on a polytetrafluorethylene membrane filter. The collected particles were extracted from the membrane using a protocol from the impactor manufacturer (BGIinc., 2008). Briefly, filters are sonicated in analysis grade methanol and the resulting dispersion is dried by vacuum evaporation. In parallel to collection, PM2.5 number size distribution and concentration were measured with high time resolution, using a scanning mobility particle sizer (SMPS) system. A section of separate filter samples was collected for chemical analysis. The PM2.5 characterization is described in detail in previous studies (Bergman et al., 2024).

The extracted particles were dispersed in ultrapure water and stored until used. Prior to treatment, the collected $PM_{2.5}$ stock was homogenized by sonication (Branson Sonifier 250), as characterised in previous protocols (Naav et al., 2020). The stock solution was then diluted in a serial dilution with Dulbecco's phosphate buffered saline (DPBS) to reach desired concentrations.

2.3 *In vitro* study design for the evaluation of dose-dependent mechanism of urban $PM_{2.5}$ exposure

To evaluate the dose-dependent effects of $PM_{2.5}$ on primary adult male HBMEC, cells were exposed to real-world equivalent concentrations of 5, 15, 75, or 300 µg/m^3 ambient $PM_{2.5}$ particles for 48h. To compare the effects of $PM_{2.5}$ exposure with ischemic-like injury, cells were designated to either normoxia, or ischemia/reperfusion injury for 3h following the first 24h particle incubation. The plates were then reperfused by incubation under physiological conditions for 24h with corresponding dose of $PM_{2.5.}$ Cell viability and oxidative stress was assessed via cell death and ROS detection assays, together with crystal violet staining for

morphological assessment. Barrier markers, inflammatory markers and LOX-1 levels was assessed through both standard western blot and in-cell western techniques. (*Figure 1*)

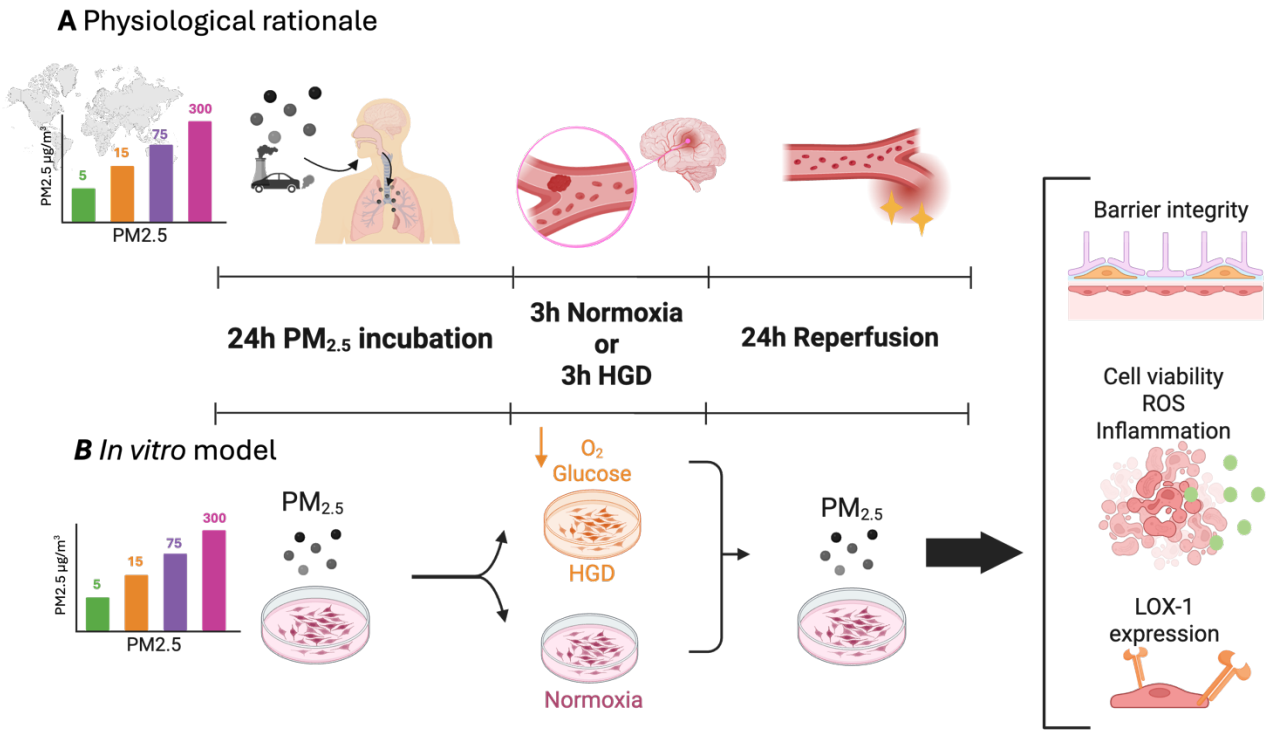

Figure 1: Study design for evaluating dose-dependent effects of particulate matter 2.5 ($PM_{2.5}$) on human brain microvascular endothelial cells (HBMEC) with *in vitro* ischemic-like injury model. A. Physiological rationale: Ambient PM2.5 exposure is epidemiologically linked to increased ischemic stroke risk. This in vitro model simulates the real-life scenario of pre-existing PM2.5 exposure followed by ischemic stroke and subsequent reperfusion. **B**. Primary adult male HBMEC were exposed to 5, 15, 75, or 300 µg/m^3 $PM_{2.5}$ for 48h in total. To compare with the effects of physiological ischemic-like injury, some plates were exposed to hypoxia (1% O_2) and glucose deprived media (HGD) for 3h after the initial 24h incubation. Following HGD or normoxia, cells were reperfused with nutrient-enriched media and incubated with $PM_{2.5}$ at normoxic (21% O_2) conditions as a reference for resolution of ischemia. Barrier integrity, cell viability, reactive oxygen species (ROS), inflammation and LOX-1 expression was assessed. Figure created in BioRender.

2.4 Cell culture and $PM_{2.5}$ treatment

Primary adult male HBMEC were purchased from Innoprot (Spain, Catalog number: P10361, Lot number: 111224CS). Cells were cultured in endothelial cell medium (Innoprot, Catalog number: P60104) according to standard protocol. All cells were treated when 85-90% confluent at passage 6-7.

HBMEC were treated with physiologically relevant equivalents of ambient exposure of 5, 15, 75 or 300 µg/m^3 $PM_{2.5}$, or 300 µg/m^3 DPBS as vehicle control. The culturing media was replaced with nutrient enriched Dulbecco's modified eagle medium (DMEM) (Gibco, Catalog

number: 21041025) together with DPBS diluted PM2.5 solution to reach the designated concentration. Plates were incubated for 48h in a CO_2 incubator at 37°C before collection.

To study physiologically relevant $PM_{2.5}$ doses within the vascular system, findings from investigations on how inhaled airborne nanomaterials interacts in the body were incorporated, which found that 1-2% of 60nm 99Tc aerosol particles were accumulated in the liver (Yacobi et al., 2011). Assuming the presence of other clearance pathways, an estimate of 3% crossing into the vasculature was assumed for this study. Additionally, an estimation of average volume of blood in human was defined to 5L. These factors were utilized to calculate the appropriate $PM_{2.5}$ concentrations representative of atmospheric exposure to $PM_{2.5}$ levels of 5, 15, 75, and 300 $\mu g/m^3$. As a result, the final concentrations of $PM_{2.5}$ within the cultures were 0.33, 0.99, 4.95, and 19.8 µg/L corresponding to the atmospheric concentrations of 5, 15, 75, and 300 $\mu g/m^3$ respectively.

2.5 *In vitro* ischemia/reperfusion injury

In vitro ischemia/reperfusion injury (HGD) was modelled based on methods of previous studies (Arkelius et al., 2024, Wendt and Gonzales, 2023). After initial 24h $PM_{2.5}$ exposure, cells designated for HGD were washed with DPBS and had their media replaced with DMEM deprived of glucose, glutamine, phenol red and sodium (Gibco, Catalog number: A1443001). The plates were then incubated in a hypoxic chamber (Stemcell technologies) flushed with a gas mixture containing 1% O_2, 5% CO_2 and nitrogen balance, in a CO_2 incubator for 3h. To simulate oxygen and nutrient reperfusion following ischemic stroke resolution, the plates were removed from the hypoxia chamber and the glucose deprived DMEM was replaced with nutrient enriched DMEM. Designated $PM_{2.5}$ concentrations were added to the plates which were then incubated in a CO_2 incubator for another 24h before analysis.

For measurement of in-cell Western, cell death, oxidative stress, and crystal violet staining, cells were seeded in 96-well plates or on glass-slides to reach a density of 1-2 x 10^4 cells and treated as described in section 2.4 and 2.5.

2.6 In-cell Western

Protein expression of tight junction proteins claudin-5 and ZO-1 was assessed with an in-cell Western kit according to manufacturer's instructions (LicorBio, Catalog number: NC2225468). 926-42094). HBMEC treated in 96-well plates were fixed with 4% formaldehyde and permeabilized with 0.1% Triton X-100. Cells were blocked with Intercept Blocking Buffer (LicorBio, Catalog number: 927-60001) and incubated with primary antibody; claudin-5 (1:200, ThermoScientific, Catalog number: 34-1600) and ZO-1 (1:200, ThermoScientific, Catalog number: 61-7300) overnight at 4°C. The cells were then washed and incubated with secondary antibody; anti-rabbit (1:1000, Li-CorBio, Catalog number: 926-3221) and CellTag520 stain (LicorBio, Catalog number: 926-41094) for 1h at RT to detect claudin-5 and cell nuclei. Fluorescent signal was measured using BMG Labtech ClarioStar Plus. Total

claudin-5 and ZO-1 protein signal was normalized to the corresponding CellTag520 stain signal. (Wendt and Gonzales, 2023)

2.7 Cell death and ROS assay

Treated HBMEC were washed with DPBS to remove excess particles. To evaluate cell death, CyQUANT cell proliferation assay was used (Invitrogen, Catalog number: C35011). A cell-permeant nucleic acid stain and a non-permeant background suppressor was incubated with the treated cells for 1h at 37°C. The plates were then imaged with an excitation and emission wavelength of 480- and 535nm respectively and a gain of 3000 (BMG Labtech, ClarioStar Plus). To assess ROS levels, dichorofluorescein diacetate (DCHF-DA) (Sigma-Aldrich, Catalog number: 35845) was dissolved in dimethyl sulfoxide (DMSO) and diluted in DPBS to a 20 μM working solution, which was then incubated with the cells for 30 min at 37°C in the dark. Following incubation, cells were washed and imaged (BMG Labtech, ClarioStar Plus) with an excitation wavelength of 485nm, emission wavelength of 520nm and gain of 2000.

2.8 Crystal violet staining

HBMEC morphology was visualized with crystal violet staining. Cells were seeded and treated on coverslips as previously described (2.4), washed, and fixed with 4% formaldehyde and incubated with crystal violet solution for 20 min at RT. The coverslips with stained cells were mounted on glass slides and imaged (Olympius Slideview VS200). Staining protocol was developed from previous studies (Wendt et al., 2021).

Cellular lengths were quantified from crystal violet images of using FIJI (ImageJ2 v2.16.0/1.54p). Prior to measurement, all images were calibrated to the spatial resolution of Olympus Slideview using the pixel size embedded in the acquisition metadata. To ensure accurate cell boundary visualization, raw images were converted to 8-bit grayscale and minimally adjusted for contrast without altering relative signal intensities. Individual cells were selected for analysis only if they were isolated, fully contained within the field of view, and not undergoing division or detachment. For each cell, its longitudinal axis was traced manually using the segmented line tool, placing sequential vertices along the central axis of the cell from one end of the membrane to the other. This approach ensured that curved or irregular cell morphologies were accurately represented. Upon completing each trace, the total path length was quantified which returned cell length in micrometers based on the previously calibrated scale.

2.9 Protein extraction and concentration determination

Treated cells were collected and combined with denaturing cell extraction buffer (ThermoScientific, Catalog number: FNN0091) containing protease- and phosphatase inhibitor (Sigma-Alrich, Catalog number: P8340, P2850). The samples were homogenized and

centrifuged to collect cell lysate. Total protein concentration was determined using a Bio-Rad protein assay (Bio-Rad, Catalog number: 5000006), measuring absorbance at 595nm on a microplate reader. Final protein concentrations were calculated from the mean absorbance value and corrected against a BSA standard curve.

2.10 Western Blot

Western Blot was run to visualize changes in protein expression of pro-inflammatory cytokine interleukin-6 (IL-6) and LOX-1 (Orset et al., 2021). Denaturing cell extraction buffer, Laemmli reagent (Bio-Rad, Catalog number: 1610737EDU) and 2-mercaptoethanol was boiled with the protein samples. Proteins were separated by SDS-PAGE on a 4-20% Tris-Glycine gel and electrotransfered to a nitrocellulouse membrane (Bio-Rad, Catalog number: 1620112). The membrane was then blocked; 5% BSA in T-TBS for IL-6, or Starting block for LOX-1 (ThermoScientific, Catalog number: 37538). Following, the membrane was incubated with primary antibody; IL-6 (1:250, Abcam, Catalog number: Ab6672) or LOX-1 (1:1000, Abcam, Catalog number: Ab60178) overnight at 4°C. Thereafter, the membrane was washed and incubated with secondary antibody; anti-rabbit (1:2000, Cell Signaling Technology, Catalog number: 7074) for 1h at RT and imaged using SuperSignal Dura kit (ThermoScientific, Catalog number: 34075) in FujiFilm LAS-1000 image analyzer. Subsequently, the membranes were stripped (ThermoScientidic, Catalog number: 21059) and probed for β-actin (1:50,000, Sigma-Aldrich, Catalog number: A3854). Signal quantification was performed using FIJI and normalized to β-actin signal as loading control. The individually loading-normalized values were then represented relative to the corresponding vehicle-treated control.

2.11 Statistical analysis

All primary HBMEC samples are replicates originating from one donor, where “n” corresponds to number of technical replicates independently repeated at least twice. Statistical analysis was performed using GraphPad Prism and all data is presented as mean ± SD. Multiple comparisons were assessed with one-way or two-way non-parametric ANOVA test (Kruskal-Wallis) and direct comparisons between two groups was assessed with Mann-Whitney test. $P < 0.05$ was considered statistically significant.

3. Results

3.1 Air $PM_{2.5}$ concentrations exceeds WHO recommendation in multiple cities globally

Of the assessed cities, Sydney had the lowest average $PM_{2.5}$ concentration of 4.3 µg/m^3 in 2024, followed by Malmö (7 µg/m^3), London (7.8 µg/m^3), Los Angeles (10.1 µg/m^3), São Paulo (15.9 µg/m^3), Beijing (30.9 µg/m^3), Kinshasa (58.2 µg/m^3) and lastly Delhi with the highest average of 108.3 µg/m^3. The WHO recommended maximum annual $PM_{2.5}$ exposure of 5 µg/m^3 is exceeded in all compared cities except for Sydney. Comparison of air pollution concentrations on November 9th or 10th of 2025 in Los Angeles, London, Malmö and Delhi shows that $PM_{2.5}$ concentrations fluctuate throughout the day in all cities. $PM_{2.5}$ in Los Angeles ranged between 12.6 and 19.6 µg/m^3, 6.0-15.3 µg/m^3 in London, 8.8-17.9 µg/m^3 in Malmö and 203-462 in Delhi. (*Figure 2*)

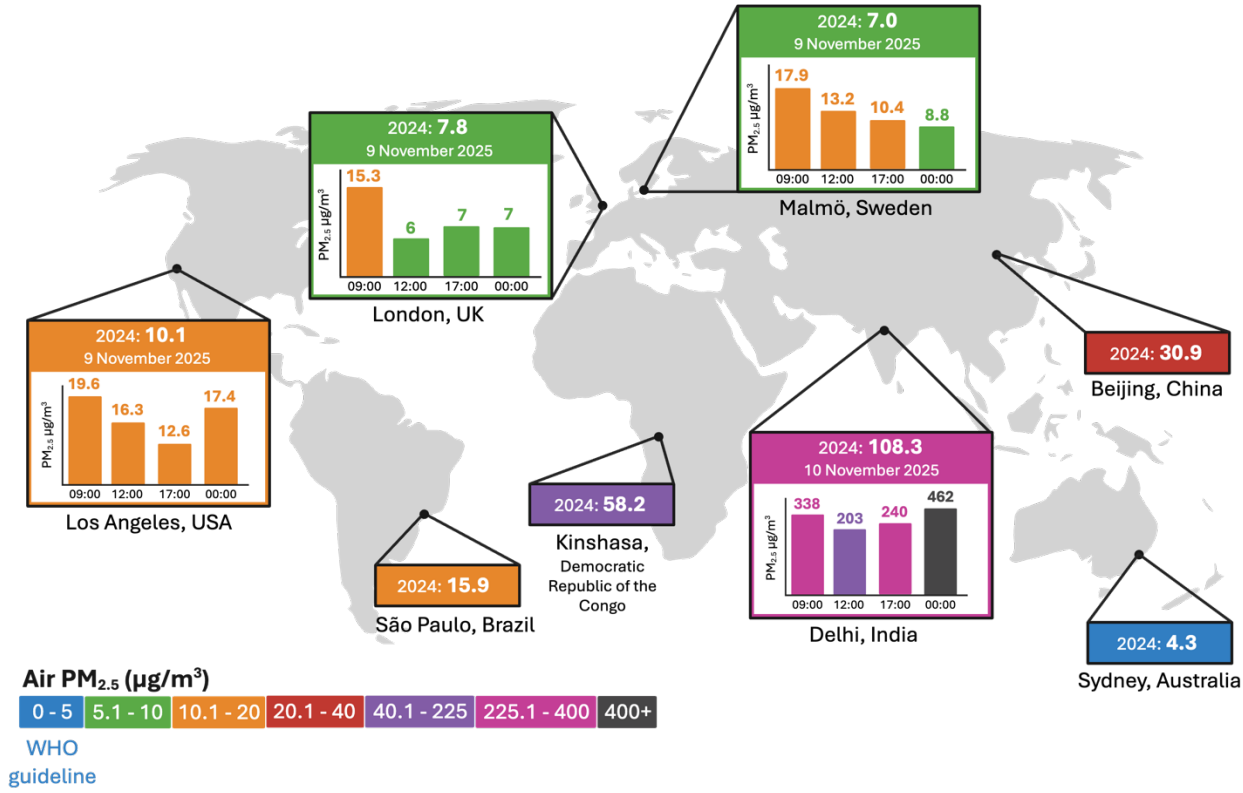

Figure 2: Comparison of atmospheric particulate matter 2.5 ($PM_{2.5}$) concentrations worldwide. Measurements of average- and daily air $PM_{2.5}$ levels in Los Angeles, São Paulo, Kinshasa, London, Malmö, Delhi, Beijing and Sydney according to IQAir 2024 world air quality report and IQAir live $PM_{2.5}$ measurement. Comparison shows that average $PM_{2.5}$ concentrations of 2024 differs drastically between cities in different areas of the world, including Sydney (4.3 µg/m^3) which is the only assessed city within the recommended WHO guideline, Malmö (7.0 µg/m^3), London (7.8 µg/m^3), Los Angeles (10.1 µg/m^3), São Paulo (15.9 µg/m^3), Beijing (30.9 µg/m^3), Kinshasa (58.2 µg/m^3) and Delhi with the highest $PM_{2.5}$ average of 108.3 µg/m^3. Data of differences in $PM_{2.5}$ concentrations during the day fluctuated in all compared cities and ranged between 12.6-19.6 µg/m^3 in Los Angeles, 6.0-15.3 µg/m^3 in London, 8.8-17.9 µg/m^3 in Malmö and 203-406 µg/m^3 in Delhi on November 9th

or 10th of 2025. Figure created in BioRender with data from iqair.com. Map lines delineate study areas and do not necessarily depict accepted national boundaries.

3.2 $PM_{2.5}$ reduces expression of BBB tight-junction proteins claudin-5 and ZO-1 in HBMEC

Total claudin-5 protein levels decreased dose-dependently with higher $PM_{2.5}$ concentration in HBMEC with in-cell western assessment from concentrations ≥15µg/m^3 compared to vehicle (*Figure 3A*). There was no difference in protein expression between $PM_{2.5}$ doses when exposed to ischemic-like injury; however, HGD exposed cells had lower protein expression in comparison to cells treated with only $PM_{2.5}$. Similarly, ZO-1 expression declined from exposure to 15- and 300µg/m^3 $PM_{2.5}$ (*Figure 3B)*. Kruskal-Wallis multiple comparison analysis of ZO-1 expression also calculated p = 0.06 between vehicle and 5µg/m^3 and p = 0.1017 between vehicle and 75µg/m^3.

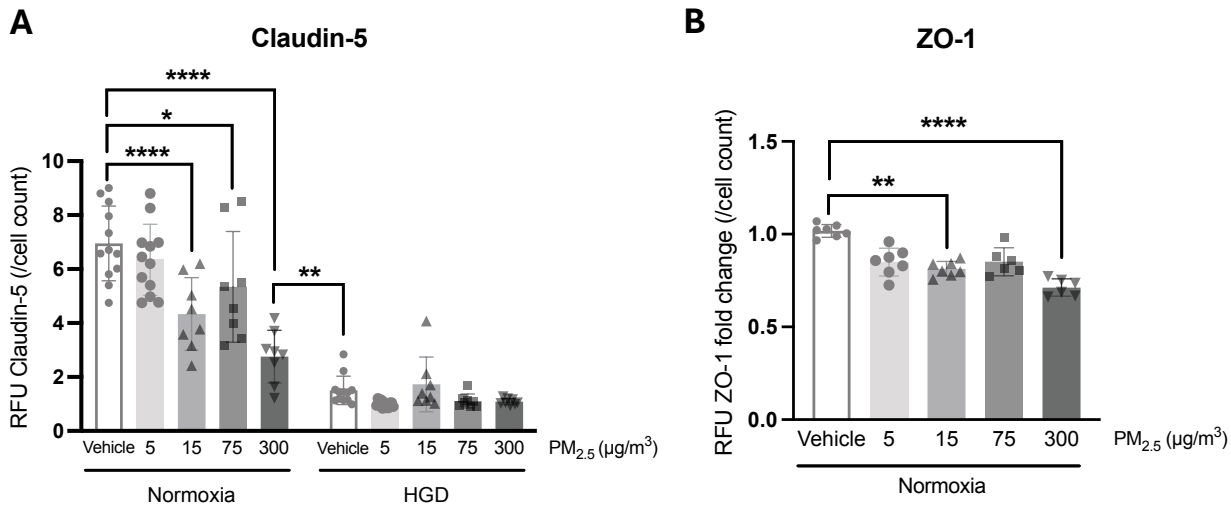

Figure 3: Decreased expression of tight-junction proteins claudin-5 and zonula occludens-1 (ZO-1) in human brain microvascular endothelial cells (HBMEC) with exposure to particulate matter 2.5 ($PM_{2.5}$). HBMEC exposed to $PM_{2.5}$ (5, 15, 75, or 300 µg/m^3) for 24h and 3h normoxia- or hypoxia with glucose deprivation (HGD) followed by 24h reperfusion. **A**. In-cell Western analysis of total claudin-5 protein expression reveals a dose-dependent decreased protein expression in normoxic cells from exposure to 15 µg/m^3 and higher. Claudin-5 levels remained constant in HGD treated cells across all $PM_{2.5}$ concentrations, however significantly lower in comparison to normoxic HBMEC. (n=12 technical replicates for vehicle and 5, n=8 technical replicates for 15, 75 and 300). **B.** In-cell Western analysis of total ZO-1 expression fold-change shows decreased protein expression from exposure to 15 µg/m^3 and 300 µg/m^3. (n=6-7 technical replicates). Data presented as mean +-SD. Statistical significance assessed through Kruskal-Wallis test within treatment groups (Normoxia/HGD) and Mann-Whitney test between groups with different treatment (300 normoxia / vehicle HGD). *p<0.05, **p<0.01, ****p<0.0001

3.3 $PM_{2.5}$ disrupts HBMEC viability and increases oxidative stress dose-dependently

Live cell count of $PM_{2.5}$ exposed HBMEC decreased dose-dependently with ascending $PM_{2.5}$ dose, from concentrations ≥75µg/m^3 compared to vehicle-treated controls (*Figure 4A*). HGD exposure significantly reduced cell viability compared to normoxic groups but showed no additional effects between exposure to different $PM_{2.5}$ concentrations. Similarly, data shows a significant dose-dependent increase in ROS levels from concentrations ≥75µg/m^3 compared

to vehicle (*Figure 4B*). HGD treatment elevated ROS levels in comparison to normoxic groups but remained stable across all $PM_{2.5}$ concentrations. Crystal violet staining and analysis of cellular length visualizes that HBMEC treated with $\geq 15 \mu g/m^3$ $PM_{2.5}$ exhibited elongated morphology in comparison to vehicle (*Figures 4C-D*). Additionally, HBMECs appeared to have erratic cellular borders which gradually extended towards neighbouring cells when exposed to higher air pollution concentrations.

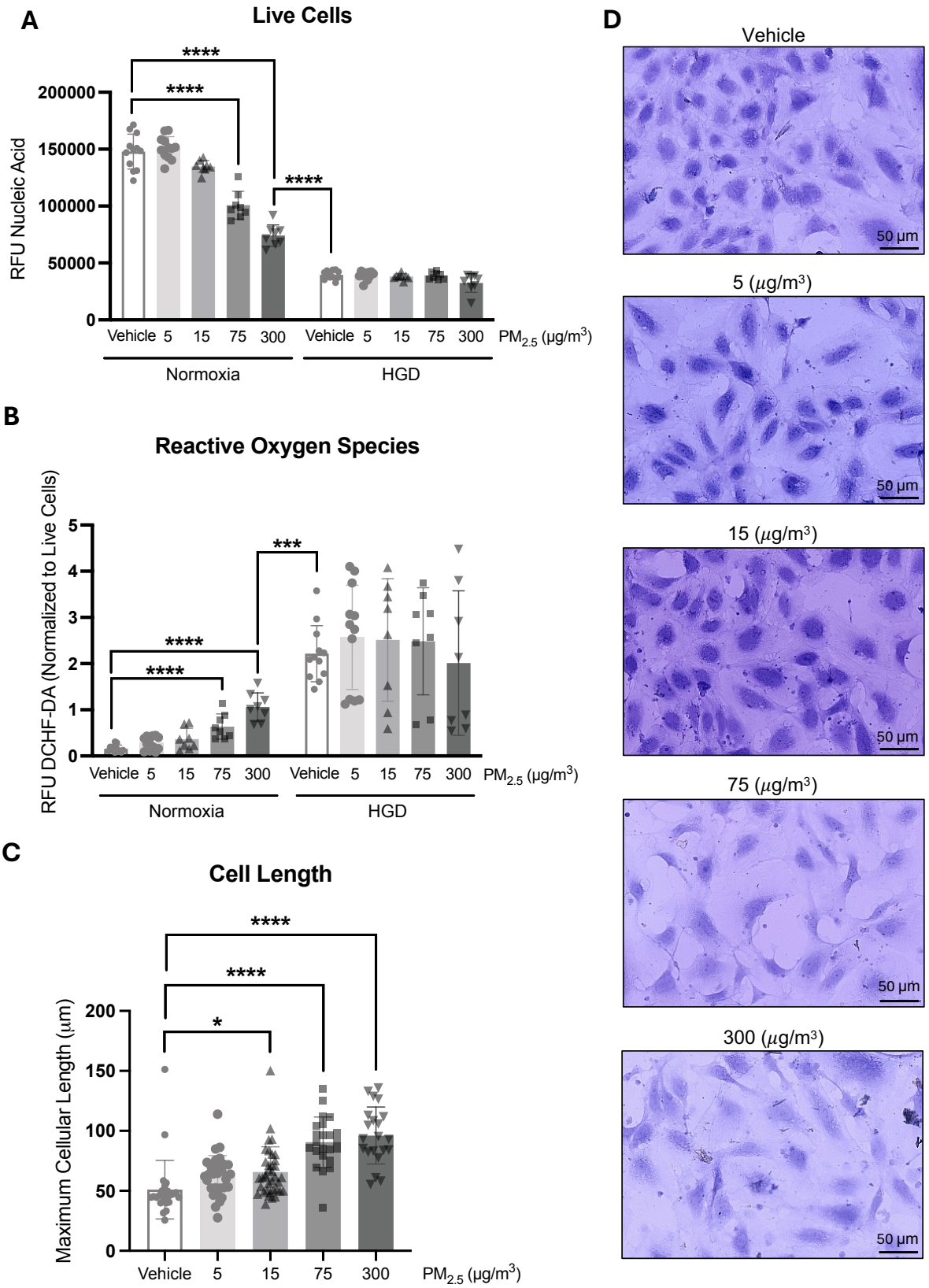

Figure 4: Differentiated live cell count, oxidative stress and cellular morphology of human brain microvascular endothelial cells (HBMEC) exposed to particulate matter 2.5 ($PM_{2.5}$) during normoxia and ischemia. Adult male HBMEC were exposed to vehicle or $PM_{2.5}$ (5, 15, 75, or 300 µg/m^3) for 24h and incubated for 3h in normoxia- or hypoxia and glucose deprivation (HGD) followed by 24h reperfusion. **A**. Live cell count (CyQUANT nuclear stain) decreased when exposed to ≥75 µg/m^3 $PM_{2.5}$ compared to vehicle. HGD treatment

reduced live cell count compared to normoxia but did not differ between particle treated groups. **B**. Reactive oxygen species (ROS) signal (DCHF-DA) normalized to live cell count. Relative ROS levels increased dose-dependently with $PM_{2.5}$ concentration, with significant increase observed at $PM_{2.5}$ ≥75 μg/m^3, in comparison to normoxia vehicle. ROS levels were uniformly elevated following HGD across all doses in comparison to normoxia vehicle and significantly higher than untreated HBMEC. (n=12 technical replicates for vehicle and 5, n=8 technical replicates for 15, 75 and 300) **C**. Analysis of crystal violet-stained HBMEC shows a longer maximum cellular length when treated with ≥15 μg/m^3 $PM_{2.5}$. (n=21-37 individual cells) **D.** Representative images of crystal violet-stained HBMEC visualizing a differentiated morphology in cells treated with higher $PM_{2.5}$ concentration, where cells appear more elongated and expanding towards neighbouring cells. Data presented as mean ± SD. Statistical significance assessed through Kruskal-Wallis test within treatment groups (Normoxia/HGD) and Mann-Whitney test between groups with different treatment (300 normoxia / vehicle HGD). *p<0.05. ***p<0.001. ****p<0.0001.

3.4 Increased IL-6 and LOX-1 protein expression from $PM_{2.5}$ exposure and *in vitro* ischemia/reperfusion injury in HBMEC

Western Blot signal quantification of pro-inflammatory cytokine IL-6 visualized no difference in 25kDa isoform between any groups (*Figures 5A-B*). However, there was a dose-dependent increase in the 17kDa isoform with $PM_{2.5}$ exposure ≥75μg/m^3 and HGD treatment compared to vehicle-treated control cells (*Figures 5A & C*). LOX-1 protein expression increased from exposure to $PM_{2.5}$ ≥15μg/m^3 and from ischemic like injury (*Figures 5D-E*).

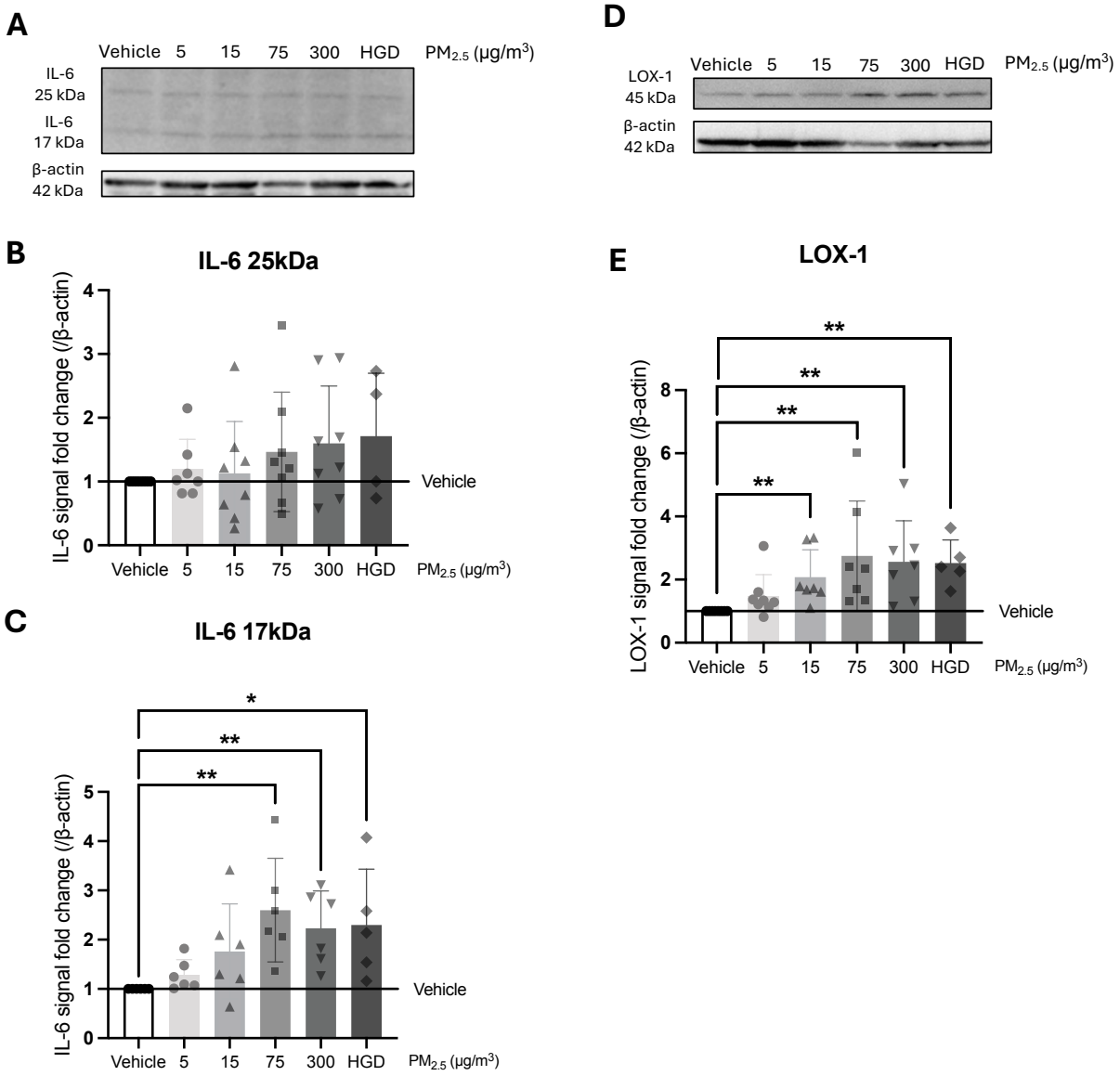

Figure 5: Dose-dependent increase in IL-6 and LOX-1 protein levels in human brain microvascular endothelial cells (HBMEC) exposed to particulate matter 2.5 ($PM_{2.5}$). Western Blot assessment of adult male HBMEC exposed to vehicle, 5, 15, 75, or 300 µg/m^3 $PM_{2.5}$ during normoxia or ischemic-like injury with hypoxia, glucose deprivation and reperfusion (HGD). **A**. Representative Western Blot image of IL-6 and β-actin band migration. **B**. Signal quantification of 25kDa IL-6 shows no difference between $PM_{2.5}$ exposure or HGD treated group. **C**. Signal quantification of 17kDa IL-6 shows dose-dependency with higher IL-6 expression from higher $PM_{2.5}$ exposure, with significant increase ≥75 µg/m^3 and from HGD treatment compared to vehicle. **D**. Representative Western Blot image of LOX-1 and β-actin. **E**. Signal quantification of LOX-1 displays a dose-dependent increase in LOX-1 with exposure to ≥15 µg/m^3 $PM_{2.5}$ or HGD. (n=4-7 technical replicates). Data presented as mean +-SD. Statistical significance assessed by Kruskal-Wallis test. *p<0.05, **p<0.01.

4. Discussion

The present study investigated the concentration-dependent effects of real-life urban $PM_{2.5}$ exposure on HBMEC, focusing on key biological mechanisms implicated in the pathogenesis of cerebrovascular diseases. Endothelial cell viability, claudin-5 and ZO-1 protein expression of the BBB, oxidative stress and inflammation were evaluated in both normoxic- and ischemic conditions. Changes in LOX-1 expression following $PM_{2.5}$ exposure was also assessed. Characterised $PM_{2.5}$ particles collected from real urban environments were applied at concentrations reflective of amounts which are realistically taken up- and reaching the cerebrovasculature via the blood circulation from environmentally relevant concentrations to higher exposure levels, thereby reflecting multiple real-world human exposure scenarios. The findings demonstrate that $PM_{2.5}$ induces clear dose-dependent alterations on the studied parameters, with notable effects on cellular morphology, claudin-5, ZO-1 and LOX-1 expression already at 15 $\mu g/m^3$, representative of conditions experienced by majority of the global population. Thus, this study addresses a critical gap in $PM_{2.5}$ research by examining environmentally and physiologically relevant concentrations at- and above the WHO's safety limit of 5 $\mu g/m^3$. This comprehensive assessment on human tissue thereby reveals the mechanistic pathways through which low-level $PM_{2.5}$ exposure may contribute to systemic and cerebrovascular disease in humans.

The present study concerns key components of the BBB, including tight-junctions and endothelial cells using human *in vitro* model. The loss of tight-junction proteins claudin-5, ZO-1 and reduced cell viability following $PM_{2.5}$ exposure was similar to the decline observed after ischemic-like injury, however, ischemia resulted in a larger loss of protein and live cells compared to only $PM_{2.5}$. Importantly, when ischemia was induced, no difference emerged between $PM_{2.5}$ concentrations, suggesting that air pollution triggers similar but less severe pathological mechanism and does not exacerbate ischemia damage once injury is initiated. Because endothelial integrity is crucial for maintaining vascular homeostasis and BBB function, its disruption increases infiltration vulnerability to cerebrovascular and neurodegenerative pathology. In stroke, BBB breakdown enables rapid influx of inflammatory cells and toxins driving neuroinflammation and brain damage (Yang et al., 2019). In Alzheimer's disease, a slower but progressive increase in barrier permeability contributes to pathological progression (van de Haar et al., 2016a, van de Haar et al., 2016b, Fiala et al., 2002). Since air pollution is associated with both stroke and neurodegenerative diseases (Kim et al., 2025, Dorsey et al., 2025), the early tight-junction breakdown and loss of endothelial barrier may be a shared mechanism by which $PM_{2.5}$ contributes to multiple cerebrovascular diseases. Additionally, the mechanism causes influx of pollution particles, directly causing neural damage (Kang et al., 2021). These findings identify $PM_{2.5}$ exposure as a risk factor for stroke induction, causing BBB dysfunction through tight-junction and endothelial damage which makes the BBB more susceptible to develop cerebrovascular diseases.

$PM_{2.5}$ exposure further reduced HBMEC viability and barrier integrity by concentration dependent increase in intracellular ROS and IL-6 release, indicating activation of oxidative

stress and inflammation. These findings of ROS and cytokine activation align with previous studies, reporting increased oxidative stress and reduced cell viability in human microvascular endothelial cells exposed to 200 μg/mL $PM_{2.5}$ and elevated IL-6 expression in lung epithelial-endothelial co-culture models exposed to 60 μg/mL $PM_{2.5}$ (Chen et al., 2017, Wang et al., 2019), which would correspond to around 2.0×10^8 and 6.0×10^7 μg/m^3 of airborne exposure, respectively. Thus, this study observes similar effects from lower $PM_{2.5}$ concentrations, in mechanisms which are central to the development of pollution-associated cardiovascular and cerebrovascular diseases. This study also concludes that LOX-1 expression increases from $PM_{2.5}$ exposure and is equally expressed from ischemic-like injury. This has been seen in the brain microvasculature of high-fat diet and apolipoprotein knock out rodents when exposed to 100 μg/m^3 diesel and gasoline exhaust (Suwannasual et al., 2018, Lucero et al., 2017), but has not been studied with $PM_{2.5}$ in healthy rodents, to our knowledge. Thereby, this study is unique in observing upregulation of a stroke-linked biomarker when exposed to as low as 15 μg/m^3 $PM_{2.5}$. Similar rodent research links diesel and gasoline particle exposure with upregulation of matrix metalloproteinases (MMPs) (Oppenheim et al., 2013), enzymes capable of degrading extracellular matrix components. Mechanistically, LOX-1 can directly upregulate MMP-9 (Li et al., 2003), a matrix metalloproteinase worsening outcome in multiple neurovascular diseases as it contributes to BBB breakdown (Rempe et al., 2016, Inzitari et al., 2013). Specifically, research point towards that MMP-9 degrades both claudin-5 and ZO-1 (Feng et al., 2011). This aligns with the findings of this study, reporting upregulation of LOX-1 and downregulation of claudin-5 and ZO-1 with 15 μg/m^3 $PM_{2.5}$, suggesting that LOX-1 mediates barrier damage from air pollution via initiating MMP production. The receptor is associated with multiple cardiovascular pathologies as it binds- and internalizes circulating oxidised low-density lipoproteins in the vascular endothelium, forming atherosclerotic plaques that can evolve into thrombi and cause both stroke and myocardial infarction (Sanchez-Leon et al., 2024). Taken together, this study suggests that LOX-1 is a key component in $PM_{2.5}$ induced endothelial damage as the receptor has downstream effects for multiple $PM_{2.5}$ associated diseases.

Global comparison of $PM_{2.5}$ concentrations show substantial variations across regions with levels fluctuating within urban areas over the course of the day. Although cities such as London and Malmö report annual averages around 7 μg/m^3 air $PM_{2.5}$ in 2024, residents are regularly exposed to over 15 μg/m^3 during morning rush hours. This indicates that residents of most surveyed cities intermittently encounter pollution concentrations capable of inducing brain endothelial damage by tight junction degradation. The ability to control and define exposure concentrations in vitro is critical, as it allows identification of dose‑response relationships and cellular thresholds for toxicity that cannot be resolved in population-based studies. While epidemiological studies associate $PM_{2.5}$ exposure with increased disease risk, most are limited by cross-sectional designs and residual confounding related to lifestyle factors and regional variability of particle composition between populations, which cannot be disregarded as potential causal components to disease development. The present findings therefore provide mechanistic insight by demonstrating that $PM_{2.5}$ directly impairs human brain endothelial function. Integrating controlled, concentration-defined experimental models with

epidemiological evidence is essential for strengthening causal inference and for informing exposure limits, risk assessment, and intervention strategies aimed at reducing the cerebrovascular health impacts of air pollution. Specifically studying and characterising $PM_{2.5}$ particles from urban environments makes the study design attributable to a larger population and not only to specific exposure areas. The collection and characterisation of $PM_{2.5}$ in this study revealed that the majority of urban particles had a diameter of less than 0.1µm, thus, ultrafine particulate matter (Bergman et al., 2024). Given that ultrafine particles can penetrate even deeper in the respiratory tract, enter the circulation, reach the cerebrovascular tract, and excert BBB disrupting effects, they are a big danger to global health. Thus, hypothesizing that ultrafine particulate matter exerts the molecular effects seen in this study. These results strengthen the current discussion in using ultrafine particulate matter as exposure metric in opposition to the current $PM_{2.5}$ (Morawska et al., 2024), as the smaller diameter penetrates deeper into physiological structures. The European Union Air Quality Directive (2024/2881) also emphasizes ultrafines as an emerging pollutant of concern (EuropeanUnion, 2024).

Since both BBB damage and LOX-1 upregulation is seen from 48h exposure to only 15 $\mu g/m^3$ $PM_{2.5}$, it is of importance to raise the question of how air pollution levels strategically can be managed to prevent disease. While the key solution is to limit air pollution exposure, it is of interest to develop a safe and effective pharmaceutical candidate to mitigate $PM_{2.5}$ induced damage when atmospheric exposure cannot be managed within the safety guidelines. Clinically, LOX-1 is mentioned as a promising therapeutic target in multiple cardiovascular diseases (Markstad et al., 2019, Arkelius et al., 2024, Schiopu et al., 2023), and inhibition of the receptor have showed promising results in phase 1 clinical trial on type 2 diabetes (Vavere et al., 2023). Given the early effects which $PM_{2.5}$ has on LOX-1 in this study, receptor inhibition may be a key in mitigating endothelial- and BBB dysfunction to prevent disease. It is thereby of further interest to investigate the role of LOX-1 in $PM_{2.5}$ induced pathogenesis, both relating to stroke and other linked diseases. Although, reducing air pollution levels is the most direct approach to avoid health effects.

In conclusion, this study highlights the critical role of environmental concentrations of $PM_{2.5}$ in mediating cellular dysfunction through impairing cell viability, inducing oxidative stress, inflammation and barrier disruption, and uniquely confirms upregulation of the scavenger receptor LOX-1 in response to air pollution exposure. These findings emphasize the cerebrovascular vulnerability to air pollution and underscore the relevance of studying $PM_{2.5}$ at a broad spectrum of physiologically relevant doses in multiple diseases which are connected to air pollution. Thus, providing valuable insights into the underlying mechanisms by which $PM_{2.5}$ contributes to the development of cerebrovascular disease.

Declaration of competing interests

The authors declare that they have no competing financial or personal interests that could have appeared to influence the work reported in this paper.

CRediT authorship contribution

Elisabet Andersson: Writing – original draft, writing – review & editing, data curation, formal analysis, investigation, methodology, visualization, validation. **Trevor Wendt**: Writing – review & editing, formal analysis, investigation, methodology, visualization, validation. **Fanny Bergman**: Writing – review & editing, investigation, methodology, resources. **Christina Isaxon**: Writing – review & editing, investigation, methodology, resources. **Saema Ansar**: Writing – review & editing, conceptualization, funding acquisition, methodology, project administration, resources, supervision.

Acknowledgements and funding sources

This work was supported by the Swedish Research Council (VR 2023-030004) (AS), Thure Carlssons Foundation (AS) and AFA (160226) (IC).

References

Arkelius, K., Wendt, T. S., Andersson, H., Arnou, A., Gottschalk, M., Gonzales, R. J. & Ansar, S. 2024. LOX-1 and MMP-9 Inhibition Attenuates the Detrimental Effects of Delayed rt-PA Therapy and Improves Outcomes After Acute Ischemic Stroke. *Circ Res,* 134**,** 954-969.

Bergman, F., Eriksson, C., Spanne, M., Ohlsson, L., Mahmutovic Persson, I., Uller, L., Rissler, J. & Isaxon, C. 2024. Physicochemical metamorphosis of re-aerosolized urban PM2.5. *Journal of Aerosol Science,* Volume 181

Best Rogowski, C. B., Bredell, C., Shi, Y., Tien-Smith, A., Szybka, M., Fung, K. W., Hong, L., Phillips, V., Jovanovic Andersen, Z., Sharp, S. J., Woodcock, J., Brayne, C., Navaratnam, A. & Khreis, H. 2025. Long-term air pollution exposure and incident dementia: a systematic review and meta-analysis. *Lancet Planet Health,* 9**,** 101266.

BGI inc. 2008. *BGI 900 Guidance manual, high volume cascade impactor*. BGI inc. https://mesalabs.com/hubfs/inmind/public/BGI900_MANUAL_1.0.0.pdf?srsltid=AfmBOoo6lm1ZPZq9vmX7ebWQ9DgzPM422jpUNYoLrImglI-_CvlLzxu0 (Accessed 23 January 2026).

Campbell, B. C. V., De Silva, D. A., Macleod, M. R., Coutts, S. B., Schwamm, L. H., Davis, S. M. & Donnan, G. A. 2019. Ischaemic stroke. *Nat Rev Dis Primers,* 5**,** 70.

Chen, S., Wu, X., Hu, J., Dai, G., Rong, A. & Guo, G. 2017. PM2.5 exposure decreases viability, migration and angiogenesis in human umbilical vein endothelial cells and human microvascular endothelial cells. *Mol Med Rep,* 16**,** 2425-2430.

Collaborators, G. B. D. S. R. F. 2024. Global, regional, and national burden of stroke and its risk factors, 1990-2021: a systematic analysis for the Global Burden of Disease Study 2021. *Lancet Neurol,* 23**,** 973-1003.

Crucet, M., Wust, S. J., Spielmann, P., Luscher, T. F., Wenger, R. H. & Matter, C. M. 2013. Hypoxia enhances lipid uptake in macrophages: role of the scavenger receptors Lox1, SRA, and CD36. *Atherosclerosis,* 229**,** 110-7.

Cui, Y., Xie, X., Jia, F., He, J., Li, Z., Fu, M., Hao, H., Liu, Y., Liu, J. Z., Cowan, P. J., Zhu, H., Sun, Q. & Liu, Z. 2015. Ambient fine particulate matter induces apoptosis of endothelial progenitor cells through reactive oxygen species formation. *Cell Physiol Biochem,* 35**,** 353-63.

Dorsey, E. R., De Miranda, B. R., Hussain, S., Bloem, B. R., Elbaz, A., Llibre-Guerra, J., Lo, R. Y., Goldman, S. M. & Tanner, C. M. 2025. Environmental toxicants and Parkinson's disease: recent evidence, risks, and prevention opportunities. *Lancet Neurol,* 24**,** 976-986.

European Union. 2024. *Directive (EU) 2024/2881 of the european parliament and of the council of 23 October 2024 on ambient air quality and cleaner air for Europe*. https://eur-lex.europa.eu/eli/dir/2024/2881/oj/eng (Accessed 2026-01-23).

Feng, S., Cen, J., Huang, Y., Shen, H., Yao, L., Wang, Y. & Chen, Z. 2011. Matrix metalloproteinase-2 and -9 secreted by leukemic cells increase the permeability of blood-brain barrier by disrupting tight junction proteins. *PLoS One,* 6**,** e20599.

Fiala, M., Liu, Q. N., Sayre, J., Pop, V., Brahmandam, V., Graves, M. C. & Vinters, H. V. 2002. Cyclooxygenase-2-positive macrophages infiltrate the Alzheimer's disease brain and damage the blood-brain barrier. *Eur J Clin Invest,* 32**,** 360-71.

Gu, Y., Hao, S., Liu, K., Gao, M., Lu, B., Sheng, F., Zhang, L., Xu, Y., Wu, D., Han, Y., Chen, S., Zhao, W., Lou, X., Wang, X., Li, P., Chen, Z., Yao, K. & Fu, Q. 2022. Airborne fine particulate matter (PM(2.5)) damages the inner blood-retinal barrier by inducing inflammation and ferroptosis in retinal vascular endothelial cells. *Sci Total Environ,* 838**,** 156563.

Gulke, E., Gelderblom, M. & Magnus, T. 2018. Danger signals in stroke and their role on microglia activation after ischemia. *Ther Adv Neurol Disord,* 11**,** 1756286418774254.

Health Effects Institute. 2025. *State of global air 2025: A report on air pollution and its role in the world's leading causes of death.* https://www.stateofglobalair.org/resources/report/state-global-air-report-2025 (Accessed 20 January 2026).

Huang, X., Steinmetz, J., Marsh, E. K., Aravkin, A. Y., Ashbaugh, C., Murray, C. J. L., Yang, F., Ji, J. S., Zheng, P., Sorensen, R. J. D., Wozniak, S., Hay, S. I., Mclaughlin, S. A., Garcia, V., Brauer, M. & Burkart, K. 2025. A systematic review with a Burden of Proof meta-analysis of health effects of long-term ambient fine particulate matter (PM(2.5)) exposure on dementia. *Nat Aging,* 5**,** 897-908.

Inzitari, D., Giusti, B., Nencini, P., Gori, A. M., Nesi, M., Palumbo, V., Piccardi, B., Armillis, A., Pracucci, G., Bono, G., Bovi, P., Consoli, D., Guidotti, M., Nucera, A., Massaro, F., Micieli, G., Orlandi, G., Perini, F., Tassi, R., Tola, M. R., Sessa, M., Toni, D., Abbate, R. & Group, M. S. 2013. MMP9 variation after thrombolysis is associated with hemorrhagic transformation of lesion and death. *Stroke,* 44**,** 2901-3.

Kadry, H., Noorani, B. & Cucullo, L. 2020. A blood-brain barrier overview on structure, function, impairment, and biomarkers of integrity. *Fluids Barriers CNS,* 17**,** 69.

Kang, K., Zhang, Y., Geng, Y., Wang, D. & Zheng, P. 2025. Andrographolide attenuates PM2.5-induced blood-brain barrier damage via antioxidant and PI3K/AKT/mTOR/NRF2 pathways. *Int Immunopharmacol,* 157**,** 114764.

Kang, Y. J., Tan, H. Y., Lee, C. Y. & Cho, H. 2021. An Air Particulate Pollutant Induces Neuroinflammation and Neurodegeneration in Human Brain Models. *Adv Sci (Weinh),* 8**,** e2101251.

Kim, B., Blam, K., Elser, H., Xie, S. X., Van Deerlin, V. M., Penning, T. M., Weintraub, D., Irwin, D. J., Massimo, L. M., Mcmillan, C. T., Mechanic-Hamilton, D., Wolk, D. A. & Lee, E. B. 2025. Ambient Air Pollution and the Severity of Alzheimer Disease Neuropathology. *JAMA Neurol,*

Krittanawong, C., Qadeer, Y. K., Hayes, R. B., Wang, Z., Thurston, G. D., Virani, S. & Lavie, C. J. 2023. PM(2.5) and cardiovascular diseases: State-of-the-Art review. *Int J Cardiol Cardiovasc Risk Prev,* 19**,** 200217.

Lee, J., Weerasinghe-Mudiyanselage, P. D. E., Kim, B., Kang, S., Kim, J. S. & Moon, C. 2023. Particulate matter exposure and neurodegenerative diseases: A comprehensive update on toxicity and mechanisms. *Ecotoxicol Environ Saf,* 266**,** 115565.

Li, D., Liu, L., Chen, H., Sawamura, T., Ranganathan, S. & Mehta, J. L. 2003. LOX-1 mediates oxidized low-density lipoprotein-induced expression of matrix metalloproteinases in human coronary artery endothelial cells. *Circulation,* 107**,** 612-7.

Li, W., Lin, G., Xiao, Z., Zhang, Y., Li, B., Zhou, Y., Ma, Y. & Chai, E. 2022. A review of respirable fine particulate matter (PM(2.5))-induced brain damage. *Front Mol Neurosci,* 15**,** 967174.

Liang, Y. Q., Kakino, A., Matsuzaka, Y., Mashimo, T., Isono, M., Akamatsu, T., Shimizu, H., Tajima, M., Kaneko, T., Li, L., Takeuchi, F., Sawamura, T. & Kato, N. 2020. LOX-1 (Lectin-Like Oxidized Low-Density Lipoprotein Receptor-1) Deletion Has Protective Effects on Stroke in the Genetic Background of Stroke-Prone Spontaneously Hypertensive Rat. *Stroke,* 51**,** 1835-1843.

Lucero, J., Suwannasual, U., Herbert, L. M., Mcdonald, J. D. & Lund, A. K. 2017. The role of the lectin-like oxLDL receptor (LOX-1) in traffic-generated air pollution exposure-mediated alteration of the brain microvasculature in Apolipoprotein (Apo) E knockout mice. *Inhal Toxicol,* 29**,** 266-281.

Markstad, H., Edsfeldt, A., Yao Mattison, I., Bengtsson, E., Singh, P., Cavalera, M., Asciutto, G., Bjorkbacka, H., Fredrikson, G. N., Dias, N., Volkov, P., Orho-Melander, M., Nilsson, J., Engstrom, G. & Goncalves, I. 2019. High Levels of Soluble Lectinlike Oxidized Low-Density Lipoprotein Receptor-1 Are Associated With Carotid Plaque Inflammation and Increased Risk of Ischemic Stroke. *J Am Heart Assoc,* 8**,** e009874.

Morawska, L., Asbach, C., Buonanno, G., Eleftheriadis,, K., F., M., Green, D., Habre, R., Harrison, Rm., Hüglin,, C., J., R., Kanninen, Km., Kumar, P., Lazaridis,, M., A., A., Querol, X., Rönkkö, T., Silvonen, V., & Stabile, L., Viana, M., Wang, H., & Wang, L. 2024. Ultrafine particle monitoring to support WHO 2021 UFP Good Practice. *European Aerosol Conference.* Tampere, Finland.

Naav, A., Erlandsson, L., Isaxon, C., Asander Frostner, E., Ehinger, J., Sporre, M. K., Krais, A. M., Strandberg, B., Lundh, T., Elmer, E., Malmqvist, E. & Hansson, S. R. 2020. Urban PM2.5 Induces Cellular Toxicity, Hormone Dysregulation, Oxidative Damage, Inflammation, and Mitochondrial Interference in the HRT8 Trophoblast Cell Line. *Front Endocrinol (Lausanne),* 11**,** 75.

Oberdorster, G., Sharp, Z., Atudorei, V., Elder, A., Gelein, R., Kreyling, W. & Cox, C. 2004. Translocation of inhaled ultrafine particles to the brain. *Inhal Toxicol,* 16**,** 437-45.

Oppenheim, H. A., Lucero, J., Guyot, A. C., Herbert, L. M., Mcdonald, J. D., Mabondzo, A. & Lund, A. K. 2013. Exposure to vehicle emissions results in altered blood brain barrier permeability and expression of matrix metalloproteinases and tight junction proteins in mice. *Part Fibre Toxicol,* 10**,** 62.

Orset, C., Arkelius, K., Anfray, A., Warfvinge, K., Vivien, D. & Ansar, S. 2021. Combination treatment with U0126 and rt-PA prevents adverse effects of the delayed rt-PA treatment after acute ischemic stroke. *Sci Rep,* 11**,** 11993.

Qin, S., Zeng, H., Wu, Q., Li, Q., Zeeshan, M., Ye, L., Jiang, Y., Zhang, R., Jiang, X., Li, M., Zhang, R., Chen, W., Chou, W. C., Dong, G. H., Li, D. C. & Zeng, X. W. 2023. An integrative analysis of lipidomics and transcriptomics in various mouse brain regions in response to real-ambient PM(2.5) exposure. *Sci Total Environ,* 895**,** 165112.

Rempe, R. G., Hartz, A. M. S. & Bauer, B. 2016. Matrix metalloproteinases in the brain and blood-brain barrier: Versatile breakers and makers. *J Cereb Blood Flow Metab,* 36**,** 1481-507.

Sanchez-Leon, M. E., Loaeza-Reyes, K. J., Matias-Cervantes, C. A., Mayoral-Andrade, G., Perez-Campos, E. L., Perez-Campos-Mayoral, L., Hernandez-Huerta, M. T., Zenteno, E., Perez-Cervera, Y. & Pina-Canseco, S. 2024. LOX-1 in Cardiovascular Disease: A Comprehensive Molecular and Clinical Review. *Int J Mol Sci,* 25

Sawamura, T., Kume, N., Aoyama, T., Moriwaki, H., Hoshikawa, H., Aiba, Y., Tanaka, T., Miwa, S., Katsura, Y., Kita, T. & Masaki, T. 1997. An endothelial receptor for oxidized low-density lipoprotein. *Nature,* 386**,** 73-7.

Schiopu, A., Bjorkbacka, H., Narasimhan, G., Loong, B. J., Engstrom, G., Melander, O., Orho-Melander, M. & Nilsson, J. 2023. Elevated soluble LOX-1 predicts risk of first-time myocardial infarction. *Ann Med,* 55**,** 2296552.

Suwannasual, U., Lucero, J., Mcdonald, J. D. & Lund, A. K. 2018. Exposure to traffic-generated air pollutants mediates alterations in brain microvascular integrity in wildtype mice on a high-fat diet. *Environ Res,* 160**,** 449-461.

Takata, F., Nakagawa, S., Matsumoto, J. & Dohgu, S. 2021. Blood-Brain Barrier Dysfunction Amplifies the Development of Neuroinflammation: Understanding of Cellular Events in Brain Microvascular Endothelial Cells for Prevention and Treatment of BBB Dysfunction. *Front Cell Neurosci,* 15**,** 661838.

Van De Haar, H. J., Burgmans, S., Jansen, J. F., Van Osch, M. J., Van Buchem, M. A., Muller, M., Hofman, P. A., Verhey, F. R. & Backes, W. H. 2016a. Blood-Brain Barrier Leakage in Patients with Early Alzheimer Disease. *Radiology,* 281**,** 527-535.

Van De Haar, H. J., Jansen, J. F. A., Van Osch, M. J. P., Van Buchem, M. A., Muller, M., Wong, S. M., Hofman, P. a. M., Burgmans, S., Verhey, F. R. J. & Backes, W. H. 2016b. Neurovascular unit impairment in early Alzheimer's disease measured with magnetic resonance imaging. *Neurobiol Aging,* 45**,** 190-196.

Vavere, A. L., Sinsakul, M., Ongstad, E. L., Yang, Y., Varma, V., Jones, C., Goodman, J., Dubois, V. F. S., Quartino, A. L., Karathanasis, S. K., Abuhatzira, L., Collen, A., Antoniades, C., Koren, M. J., Gupta, R. & George, R. T. 2023. Lectin-Like Oxidized Low-Density Lipoprotein Receptor 1 Inhibition in Type 2 Diabetes: Phase 1 Results. *J Am Heart Assoc,* 12**,** e027540.

Wang, G., Zhang, X., Liu, X., Zheng, J., Chen, R. & Kan, H. 2019. Ambient fine particulate matter induce toxicity in lung epithelial-endothelial co-culture models. *Toxicol Lett,* 301**,** 133-145.

Wendt, T. S. & Gonzales, R. J. 2023. Ozanimod differentially preserves human cerebrovascular endothelial barrier proteins and attenuates matrix metalloproteinase-9 activity following in vitro acute ischemic injury. *Am J Physiol Cell Physiol,* 325**,** C951-C971.

Wendt, T. S., Li, Y. J. & Gonzales, R. J. 2021. Ozanimod, an S1PR(1) ligand, attenuates hypoxia plus glucose deprivation-induced autophagic flux and phenotypic switching in human brain VSM cells. *Am J Physiol Cell Physiol,* 320**,** C1055-C1073.

World Health Organization. 2021. *WHO global air quality guidelines: Particulate matter (PM(2.5) and PM(10)), ozone, nitrogen dioxide, sulfur dioxide and carbon monoxide*. Geneva. https://www.ncbi.nlm.nih.gov/pubmed/34662007 (Accessed).

World Health Organization. 2022. *Billions of people still breathe unhealthy air: new WHO data*. https://www.who.int/news/item/04-04-2022-billions-of-people-still-breathe-unhealthy-air-new-who-data (Accessed 14 November 2025).

World Health Organization. 2024. *Ambient (outdoor) air pollution*. https://www.who.int/news-room/fact-sheets/detail/ambient-(outdoor)-air-quality-and-health (Accessed 14 November 2025).

Yacobi, N. R., Fazllolahi, F., Kim, Y. H., Sipos, A., Borok, Z., Kim, K. J. & Crandall, E. D. 2011. Nanomaterial interactions with and trafficking across the lung alveolar epithelial barrier: implications for health effects of air-pollution particles. *Air Qual Atmos Health,* 4**,** 65-78.

Yang, C., Hawkins, K. E., Dore, S. & Candelario-Jalil, E. 2019. Neuroinflammatory mechanisms of blood-brain barrier damage in ischemic stroke. *Am J Physiol Cell Physiol,* 316**,** C135-C153.

Zhu, X. M., Wang, Q., Xing, W. W., Long, M. H., Fu, W. L., Xia, W. R., Jin, C., Guo, N., Xu, D. Q. & Xu, D. G. 2018. PM2.5 induces autophagy-mediated cell death via NOS2 signaling in human bronchial epithelium cells. *Int J Biol Sci,* 14**,** 557-564.